

# A modular computational circulatory model applicable to VAD testing and training

Gianfranco Ferrari · Maciej Kozarski · Krzysztof Zieliński · Libera Fresiello · Arianna Di Molfetta · Krystyna Górczyńska · Krzysztof J. Pałko · Marek Darowski

Received: 15 February 2011 / Accepted: 26 August 2011 / Published online: 20 September 2011  
© The Japanese Society for Artificial Organs 2011

**Abstract** Aim of this work was to develop a modular computational model able to interact with ventricular assist devices (VAD) for research and educational applications. The lumped parameter model consists of five functional modules (left and right ventricles, systemic, pulmonary, and coronary circulation) that are easily replaceable if necessary. The possibility of interacting with VADs is achieved via interfaces acting as impedance transformers. This last feature was tested using an electrical VAD model. Tests were aimed at demonstrating the possibilities and verifying the behavior of interfaces when testing VADs connected in different ways to the circulatory system. For these reasons, experiments were performed in a purely numerical mode, simulating a caval occlusion, and with the model interfaced to an external left-VAD (LVAD) in two different ways: with atrioaortic and ventriculoaortic connection. The caval occlusion caused the leftward shift of the LV  $p$ - $v$  loop, along with the drop in arterial and ventricular pressures. A narrower LV  $p$ - $v$  loop and cardiac output and aortic pressure rise were the main effects of

atrioaortic assistance. A wider LV  $p$ - $v$  loop and a ventricular average volume drop were the main effects of ventricular-aortic assistance. Results coincided with clinical and experimental data attainable in the literature. The model will be a component of a hydronumerical model designed to be connected to different types of VADs. It will be completed with autonomic features, including the baroreflex and a more detailed coronary circulation model.

**Keywords** Lumped parameter model · Computational model · Cardiovascular system · Ventricular elastance · Heart assist device

## Introduction

Modeling can be a powerful tool for analyzing complex interactions among the heart (in the case of a residual heart contractility), the circulatory system, and the assist device [1, 2], especially when mechanical circulatory assistance is aimed at heart recovery. The advantages of modeling lie in the possibility of analyzing the sensitivity of several circulatory and ventricular variables to the mechanical circulatory assistance and, conversely, the effects of selected circulatory and ventricular parameters on the assistance performance. Of course, the model, to be really effective, should be capable of reproducing the interaction between the circulatory system and the assist device in different conditions. The key point is the assist device: in fact, if it is modeled and connected to a circulatory model, the device would be represented as a computational model that is, by definition, an approximate representation of the original. If, on the contrary, the assist device itself is used, it should be connected to a circulatory model that is, e.g., hydraulic—again being an approximate representation of the original,

---

G. Ferrari (✉) · L. Fresiello (✉) · A. Di Molfetta  
Institute of Clinical Physiology, Section of Rome,  
CNR, Via San Martino della Battaglia 44,  
00185 Rome, Italy  
e-mail: gfr.ferrari@ifc.cnr.it

L. Fresiello  
e-mail: libera.fresiello@gmail.com

M. Kozarski · K. Zieliński · K. Górczyńska ·  
K. J. Pałko · M. Darowski  
Institute of Biocybernetics and Biomedical Engineering,  
PAN, Warsaw, Poland

A. Di Molfetta  
Department of Cardiology, Tor Vergata University,  
Rome, Italy

in this case, the circulatory system. It is worthwhile to mention that in general, a hydraulic model is less accurate and more expensive than a computational model. On the other hand, the model limitations in testing real devices with sufficient accuracy are one of the reasons experiments on animals, despite their limitations (costs, ethical problems and intrinsic randomness of biological systems), are still widely used.

Several research groups tried to solve the apparently unsolvable dichotomy between computational and hydraulic models and between accuracy and the possibility of using real devices. Some of them developed the idea to merge computational and hydraulic models [3–5] to test mechanical heart assist devices in conditions as close as possible to the real ones. Many attempts performed so far focused on the realization of single components merging computational and hydraulic features [3, 6–8]. Another possible approach is to use a comprehensive computational circulatory model, “interfaceable” if necessary with different environments, to create the prerequisites to test mechanical heart assist devices [9]. This approach seems to be more appealing for research, training, and educational purposes; furthermore, it permits use of the same model for many different applications.

The aim of this paper is to describe a computational circulatory model designed for use in different pathophysiological conditions, including its connection with a mechanical heart assist device. The latter is simplified here to verify the model’s capability to react to assistance by an electrical model. This seems to contradict what was stated above. However, despite being a model of the device, an electrical model is developed in an environment different from the computational one and permits fast and inexpensive testing of all connections between the two environments, verifying at the same time the model’s reaction to mechanical circulatory assistance modeled as a physical device.

**Materials and methods**

The lumped parameter circulatory model and its structure

The modular circulatory model is an evolution of a previous one [10] and is characterized by a high degree of flexibility and a polymorphic structure, easy adaptation to the model for different experimental needs, including the presence of ventricular assist devices (VADs). In this way the modeling system opens a window on the physical environment when and if necessary. The closed-loop model (Fig. 1) is divided into five functional modules: left and right ventricles, systemic circulation (arterial and venous),

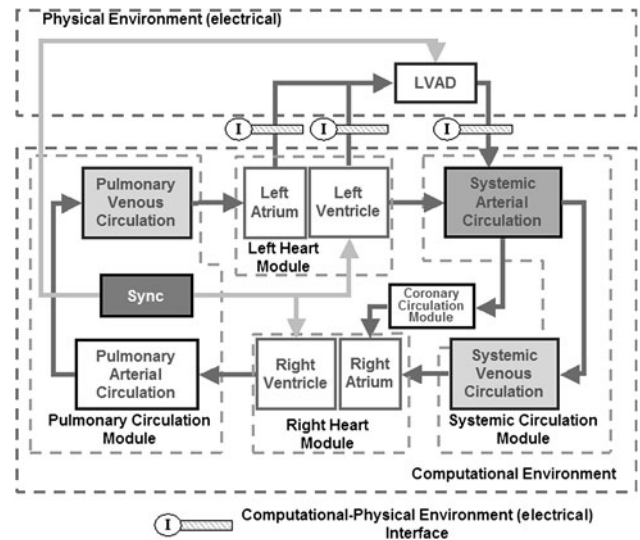


**Fig. 1** Modular circulatory model. Presence of the interface (I) means that the numerical model was interfaced with an assist device. Connections of coronary circulation module evidence blood-flow direction, not functional relationships. The block SYNC generates a trigger signal, usable inside and outside the computational model, at the beginning of each cardiac cycle

pulmonary circulation (arterial and venous), and coronary circulation. Each module embeds a library of models that can be chosen according to the experimental needs. The computational model equations, solved using Euler’s method, are organized in such a way that for each block (or subblock, if any), the pressure ( $P$ ) inside the block and the input flow ( $Q_{in}$ ) to the next one are calculated according to Eqs. 1–5 written for a generic RLC block (see Fig. 2):

$$Q_{in\ n}(t) = Q_{Cn}(t) + Q_{out\ n}(t) \tag{1}$$

$$P_{n-1}(t) - P_n(t) = L_n \cdot \frac{dQ_{in\ n}(t)}{dt} + Q_{in\ n}(t) \cdot R_{n1} \tag{2}$$

$$Q_{Cn}(t) = C_n \cdot \frac{dP_n(t)}{dt} \tag{3}$$

$$Q_{out\ n}(t) = Q_{in\ n+1}(t) \tag{4}$$

$$Q_{in\ n+1}(t) = \frac{(P_n(t) - P_{n+1}(t))}{R_{n2}}, \tag{5}$$

where  $Q_{in\ n}$  is the input flow into the block  $n$  (previously calculated in the block  $n - 1$ ),  $Q_{out\ n}$  is the output flow from block  $n$  corresponding to input flow  $Q_{in\ n+1}$  into the block  $n + 1$ ,  $P_{n-1}$ ,  $P_n$  and  $P_{n+1}$  are the pressures in block  $n - 1$ ,  $n$  and  $n + 1$ , respectively. Equation 2 is solved to calculate  $Q_{in\ n}$  ( $Q_{out\ n-1}$ ), whereas  $P_n$  is calculated solving Eqs. 1 and 3.  $R_{n1}$ ,  $R_{n2}$ ,  $L_n$ ,  $C_n$  represent resistive, inertial and capacitive elements of the block  $n$ , respectively. Heart rate (HR) controls timing in the model (Fig. 1) and is set manually in the control panel (see below, software package). A trigger signal (SYNC) is generated at the beginning

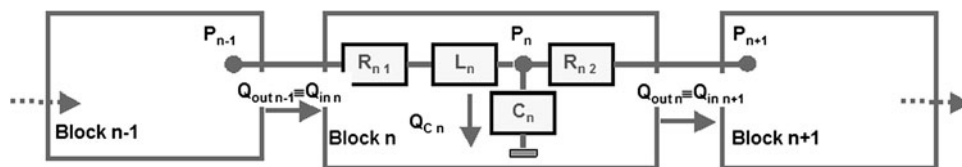


**Fig. 2** Relationship among three consecutive generic RLC blocks in the model. Each block calculates a pressure, receives input flow from the previous one, and transmits input flow to the next one

of ventricular contraction and is used to synchronize external devices such as VADs.

As shown in Fig. 1, the model can be connected to a left-VAD (LVAD), pulsatile in this study. This feature will be described in one of the next paragraphs. A short description of the library models used in this paper or available for each module from Fig. 1 follows (a glossary of terms is presented in Table 3 in Appendix):

#### *Left and right heart chambers*

**Left–right ventricles** Right and left ventricular systolic phases are represented using two variable elastance models [11, 12], whereas the corresponding diastolic phases are represented as a sum of exponentials [13]. Passage from ejection phase to filling phase is controlled by the systole/diastole ratio (S/D) that can be set manually or automatically generated as a function of HR. Connection of the ventricle to the circulatory network is achieved via valves, which are assumed to be ideal: when the valves are open, the flow through is proportional to the pressure drop; when closed the flow is equal to zero. The library also includes two more complex models of valves. The first is achieved by improving on the previous model, including an inverse resistance that simulates the presence of retrograde flow. The second permits description of valves leaflet motion, relating them to the cardiac cycle. In particular, valve lumens change as a function of pressures and leaflet properties [14]. The library includes a version of the variable elastance model governed by electrocardiographic (ECG) signal and a partialized version of the ventricles, including intraventricular septum, which simulates complex ventricular pathologies [15].

**Left–right atria** In the discussed model, atria are passive elements, and each is represented by a single compliance. However, the model library contains an active version of atria, governed by ECG [15], which is especially useful to simulate the effects of atrioventricular dyssynchrony.

#### *Systemic circulation (arterial–venous)*

We present two models from this library. The first is composed of a four-element windkessel (arterial) used in

hybrid applications, together with a two-element windkessel representing venous circulation. The second is derived from a more complex model [16] and is essentially based on the division of systemic circulation into upper and lower body (Fig. 3). Two subblocks ( $Z_1$ ,  $Z_2$ ), including ascending aorta, aortic arch, and thoracic–abdominal aorta, respectively, represent the aorta itself. The lumped elements were calculated by simplifying a lumped model of the aorta [17]. Values were chosen preserving input impedance of the arterial system.

#### *Pulmonary circulation (arterial–venous)*

Arterial circulation is represented by a modified windkessel and venous circulation by a simple windkessel [10].

#### *Coronary circulation*

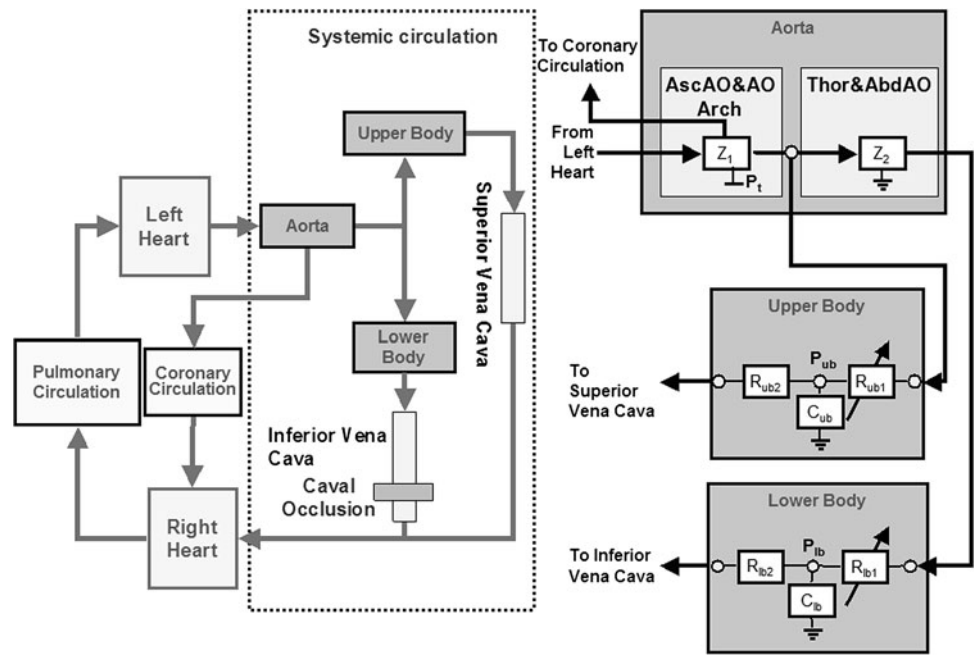
Coronary circulation is simulated by a simple model [18] represented by a single resistive branch polarized by LV pressure. The model library contains a more complex coronary circulation model, including common trunk, right coronary, circumflex, and anterior descending arteries.

Values of all lumped parameters used in the model are given in Table 3 in the Appendix. The model has an additional feature: intrathoracic pressure is represented by the variable  $P_t$  to simulate the effect spontaneous breathing or lung ventilation on hemodynamics [19]. By setting  $P_t$  to zero, an open-chest condition is simulated. It is also possible to change the pressure  $P_t$  in a sinusoidal manner to reproduce the time-varying effects of respiration, if necessary.

#### *Software package*

The model was developed in LabVIEW(National Instruments, Austin, TX, USA) environment (Release 7.1 for Windows). Differential equations describing the model were solved using Euler's method with a default time interval of 1 ms. Software is based on three nested cycles: the internal one is a FOR cycle and solves the equations within the cardiac cycle as well as performing point-by-point buffered data presentation and average (in the cardiac cycle) variables calculation. The second nested cycle is a WHILE loop and performs several tasks:

**Fig. 3** Systemic circulation module split into upper- and lower-body circulation.  $Z_1$  and  $Z_2$  include inertial, capacitive, and resistive components of the two blocks representing aorta. Two RC cells represent superior and inferior vena cava. The block labeled *caval occlusion* is used to reproduce the corresponding maneuver and demonstrate the meaning of end-systolic pressure–volume relationship (ESPVR) line



- switches from one cardiac cycle to the next;
- generates a periodic trigger pulse (period equal to cardiac cycle duration) determining the beginning of ventricular ejection;
- receives user inputs.

Finally, the third nested cycle is a WHILE loop and is used for error management and system reset to default conditions. The same software is also used for applications aimed at testing mechanical circulatory assistance (see “Mechanical assistance and computational–electrical connections”) and includes routines for real-time operations and error management. Special attention was devoted to developing the graphical user interface [10]. It is based on a control panel composed of three subpanels (user interface, main controls and data presentation, secondary controls); each contains different levels of simulation controls and presentations. The main panel presents essential information (ventricular- and aortic-pressure time courses, ventricular pressure–volume loops) and gives access to some subpanels controlling the different applications. Two of the subpanels permit starting and controlling LVAD assistance and the caval occlusion maneuver, respectively.

**Mechanical assistance and computational–electrical connections**

A multienvironment model, computational–physical in this case, is based on real-time exchange of data between its computational and physical components. The connection between computational and physical parts of the model is performed via an interface. In the case of lumped

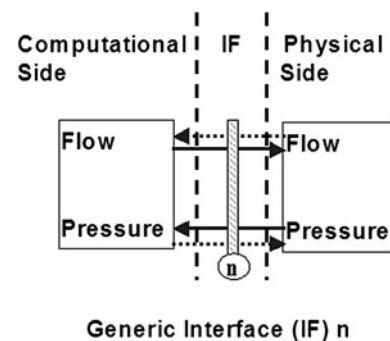


**Fig. 4** Role of interfaces in data exchange between the two modeling environments. The variable exchange is symmetric in both directions: if flow is calculated in the computational side, a pressure is acquired in the physical side (solid arrows) and vice versa (dashed arrows)

parameter models, the interface should permit exchange of two variables, as is schematically shown in Fig. 4, where the solid and dashed arrows evidence the possible variable exchanges. If a flow is calculated in the computational side, a pressure is acquired in the physical side and vice versa.

Functionally, the first variable (pressure or flow) is acquired in the physical side, converted, and used to solve equations in the numerical side. The second variable (flow or pressure) is calculated in the numerical side, converted, and applied to the physical section. One advantage of these principles is their applicability to any physical structure (hydraulic, electrical) [9, 20]. The interfaces between computational and physical parts of the model are based on the concept of impedance transformers [21]. These four-terminal blocks transmit and transform the signals connecting the two environments: numerical and physical

(hydraulic or electrical). Impedance transformers therefore embed numerical and physical terminals. The pair of physical variables (hydraulic pressure drop and flow or voltage and current) in physical terminals is converted into directly proportional corresponding variables (numerical pressure drop and flow) at the numerical terminals and vice versa. Finally, impedance “seen” at the physical terminals is exactly proportional to impedance “seen” at the numerical terminals.

Timing is a critical issue in a model merging computational and physical environments. It is fundamental that a numerical sample corresponds exactly to a physical sample. This problem is solved exploiting the basic structure of the software using each step of the internal FOR loop for analog to digital (A/D) and D/A conversions [input/output (I/O) board, PCI-MIO-16E–4 National Instruments]. The duration of each step is equal to the time interval used for Euler’s method equation solving. Numerical and physical data are therefore synchronized within a time uncertainty equal to the set time interval (default 1 ms). Thanks to the software’s modular structure, it is enough to replace the calculated variable with the physical variable and insert it into the data-flow paths. An example can explain the last assertion: if the systemic arterial windkessel has to be replaced with a physical circuit, the calculated output flow from the LV is used as an input to the physical circuit. From the physical circuit, in turn, a variable is acquired (arterial pressure in our example) to be used in the model equations. Of course, a closed-loop circuit, as in the case of our circulatory model, needs a second interface at the physical circuit output, where flow is acquired and used inside the model equations to calculate the pressure in the next block after the physical circuit [9]. A similar approach can be used in the case of LVAD assistance with atrioaortic and ventriculoaortic connection, as shown in Fig. 5a, b. The interfaces are used to transmit an output variable (pressure or flow) to the physical LVAD and to receive from it an input variable flow or pressure, respectively. Left atrial pressure ( $P_{la}$ ) or ventricular pressure ( $P_{lv}$ ) are the output variables of the model and the input variables of the LVAD, determining its filling.  $Q_{inVAD}$ , measured and acquired in the physical LVAD, is used to solve the equations of left atrial (Eq. 6) or ventricle (Eqs. 7a, 7b) nodes, depending on the way of connection (Fig. 5):

$$Q_{vp}(t) = C_{la} \cdot \frac{dP_{la}(t)}{dt} + Q_{inVAD}(t) + Q_{li}(t) \quad (6)$$

$$P_{lv}(t) = E_{lv}(t) \cdot (V_{lv}(t) - V_0) \quad (7a)$$

$$\frac{dV_{lv}(t)}{dt} = Q_{li}(t) - Q_{inVAD}(t) - Q_{lo}(t) \quad (7b)$$

Equation 7a is used to evidence the relationship among ventricular node variables. The equation represents the

ventricular variable elastance model in its simplest form and does not include ventricular filling relationship. Systemic arterial pressure  $P_{as}$  is applied at the LVAD output terminal and determines LVAD output flow  $Q_{outVAD}$ , which is acquired and used to solve the equation (Eq. 8) of the systemic arterial node (Fig. 5):

$$C_{as} \cdot \frac{dP_{as}(t)}{dt} = Q_{lo}(t) + Q_{outVAD}(t) - Q_{as}(t) - Q_{cor}(t) \quad (8)$$

Variables acquired in the physical part of the model are bolded in Eqs. 6–8. As this approach can be indifferently applied to physical hydraulic or electrical circuits/devices, the electrical physical circuits can be used to prove validity of a model, to develop its software, and for educational purposes. In this project, we used a physical–electrical LVAD to verify the feasibility of merging different environments, comparing atrioaortic and ventriculoaortic assistance connections. The LVAD physical–electrical model is rather simple and is shown schematically in Fig. 6a, b. It is based on the principle that external pressures ( $P_{la}$  and  $P_{as}$ ) interact with VAD internal pressure and provoke VAD I/O valves opening and closing. Two interfaces (voltage-controlled voltage generators; VCVG [20]), playing the role of impedance transformers, connect the physical electrical device to the numerical circulatory model. Voltage, proportional to atrial -①-, ventricular -②-, and aortic -③- pressures, is applied at both ends of the physical electrical LVAD. The LVAD is built of three main functional blocks: input and output valves (represented by operational amplifier diodes) and a programmable function generator (Arbitrary waveform generator model 75, Wavetek, San Diego, CA, USA) producing a voltage signal. This voltage signal, equivalent to a pressure, permits LVAD filling and emptying on the basis of pressure signals applied to its input and output terminals. The function generator is programmed through the general-purpose interface bus (GPIB) (PCI GPIB board, National Instruments) and is triggered by the SYNC signal generated by the software through the digital output (dig-out) board (I/O board PCI-MIO-16E–4). Gains for two pressures transmitted to the physical electrical LVAD are regulated to get equal LVAD input and output flows. The two VCVG interfaces are used to read LVAD input and output flows by measuring two currents [20] from the voltage drop in resistance R10 in Fig. 6b.

#### Experimental method

The aim of this paper is to describe the flexibility of the modular computational circulatory model software and its capability to reproduce human-like hemodynamic

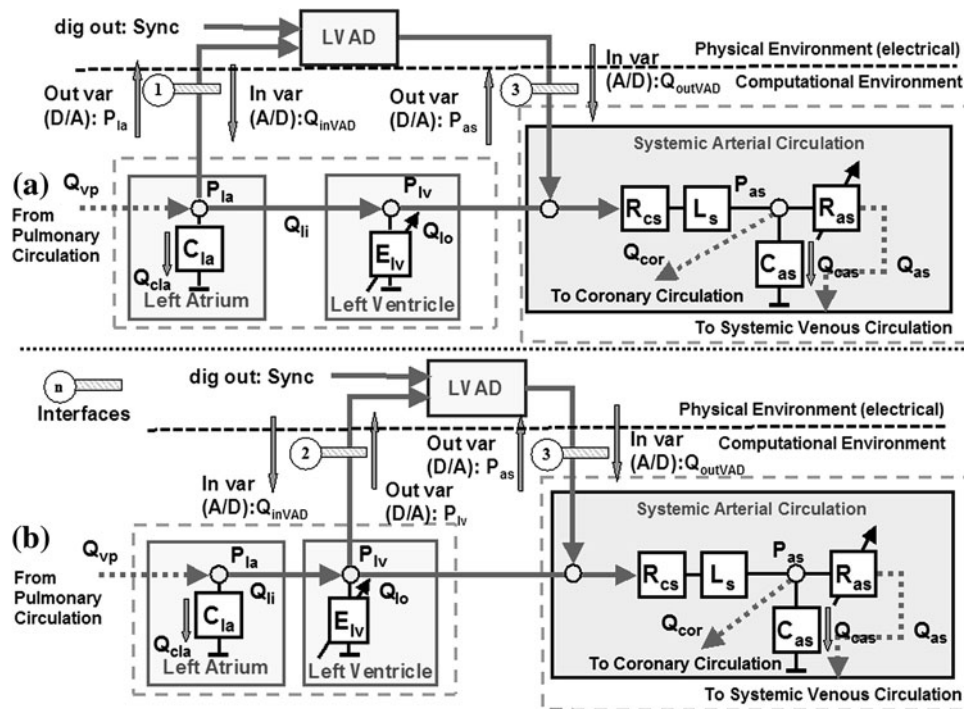


**Fig. 5** Connections between the computational model and the left ventricular assist device (LVAD). Physical and computational variables are indicated. **a** Interfaces ① and ③ correspond to the atrioaortic connection. Arrows placed at both sides of each interface indicate model input (flow) and output (pressure) variables. Model input at interface ① is LVAD input flow; model output at the same interface is left atrial pressure. Model input at interface ③ is LVAD

output flow; model output at the same interface is systemic arterial pressure. **b** Interfaces ② and ③ correspond to ventriculoaortic connection. Arrows placed at both sides of each interface indicate model input (flow) and output (pressure) variables. Model input at interface ② is LVAD input flow; model output at the same interface is LV pressure. Model input at interface ③ is LVAD output flow; model output at the same interface is systemic arterial pressure

conditions in both purely computational and computational–physical modes when interfaced, in the latter case, to a physical LVAD. To this aim, the model was used in numerical mode to reproduce a caval occlusion maneuver using the systemic circulation model described in Fig. 3, as this configuration permits reproduction of an occlusion of the inferior vena cava. The computational–physical mode experiments were performed exploiting the model configuration from Fig. 1, where the systemic arterial tree was represented by a modified windkessel. In this case, a simpler arterial model was enough to test the mutual influences among the heart, the arterial system, and the assist device. The model was connected to the electrical LVAD both in atrioaortic and ventriculoaortic modes according to the schema of Fig. 5.

*Caval occlusion*

The caval occlusion maneuver is routinely used to evaluate end-systolic ventricular elastance. It is achieved by clamping the inferior vena cava and progressively reducing venous return. As a consequence, LV *p–v* loop shifts leftwards on the *p–v* plane. The line joining the points identified by ventricular end-systolic pressure and volume

represents ventricular end-systolic elastance. Inferior vena cava occlusion (grey rectangle in Fig. 3) was achieved by raising the resistive component in the inferior vena cava model (represented by an R–C cell).

*LVAD assistance*

Atrioaortic and ventriculoaortic LVAD pulsatile assistance [10, 22] was reproduced on the model, and in both cases, the pre-LVAD hemodynamic condition was used as a control (see the Left heart and Right heart columns in Table 1). Next, the LV was assisted using both types of assistance synchronously.

Results of both experiments are presented in the form of data averaged in the cardiac cycle and as ventricular *p–v* loops. Table 1 presents the main circulatory and ventricular parameter settings, including LV and RV end-systolic elastance  $E_{max}$  and rest volume  $V_0$ , for all experiments performed and discussed. All circulatory parameters were calculated or estimated from experimental and clinical data and were used to set the model. In particular, the set of columns marked as Systemic circulation-1 includes the parameters of the configuration used for LVAD atrioaortic and in ventriculoaortic connection assistance. The

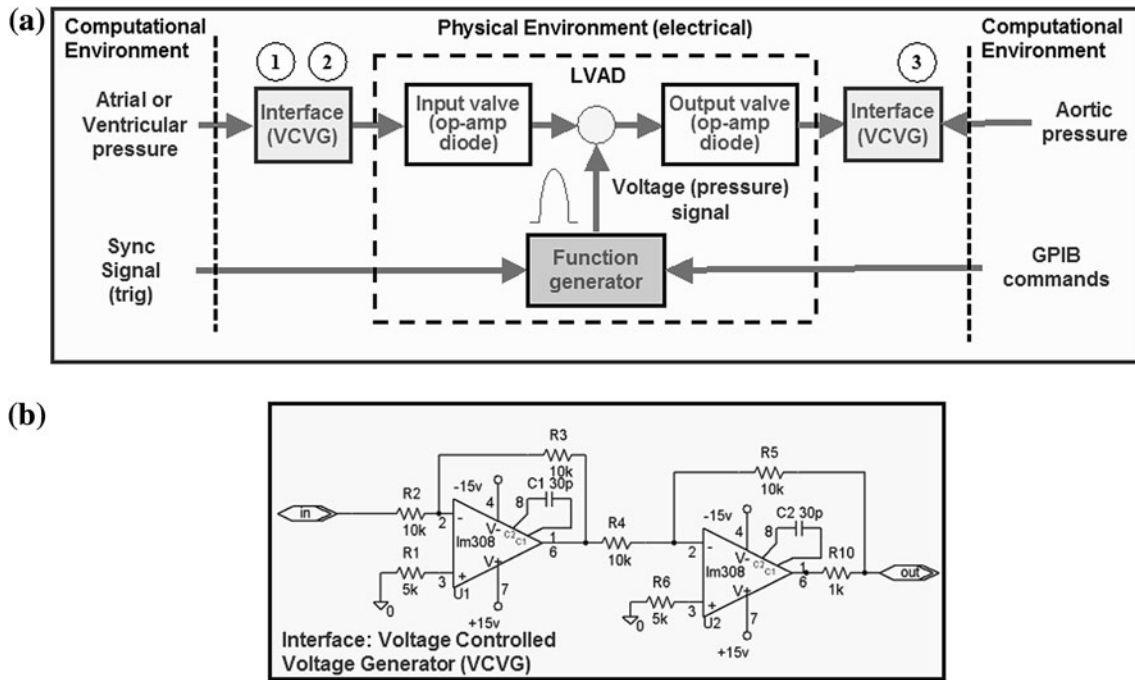


**Fig. 6** Physical–electrical left-ventricular device (LVAD) and voltage-controlled voltage generators (VCG) interface. **a** LVAD and interfaces for computational–physical environments connection. LVAD is composed of three functional blocks: input and output valves (attained via operational amplifier diodes) and a programmable voltage generator triggered by the SYNC signal coming from the

computational model. The voltage generator is controlled by a general-purpose interface bus (GPIB). **b** Electrical schematics of voltage-controlled voltage generator (VCG) interface. Each interface is composed of two operational amplifiers, and LVAD input and output flows are measured on resistance R10

set of columns marked as Systemic circulation-2 contains the parameters for the caval occlusion experiment (see Fig. 3 for reference).

## Results

Results obtained during the caval occlusion maneuver are reproduced in Fig. 7: Panel a shows the LV and systemic arterial pressures time courses. Panel b presents the LV  $p$ – $v$  loops during occlusion development (every fifth cycle of this process is presented). The working points, moving from position  $P_1$  to  $P_7$ , identify the end-systolic pressure–volume relationship (ESPVR) line of the LV.

Figures 8a, b and 9a, b show the time courses of LV and aortic pressures, along with the LVAD output flow (panel a) and the ventricular  $p$ – $v$  loops (panel b) in the case of atrioaortic and ventriculoaortic connection LVAD assistance. Each panel shows control (before LVAD assistance onset) and assisted time courses and  $p$ – $v$  loops.

The values of hemodynamic variables corresponding to the performed LVAD assistance simulation are resumed in Table 2 where they are compared with some clinical experimental results attainable from the literature [8, 22].

## Discussion

Simulation results obtained from the model in both computational and computational–electrical configurations are in good accord with clinical and experimental data. The experiments described here deserve some comments. The caval occlusion maneuver demonstrates the flexibility of the model and its educational potential to explain some fundamental hemodynamic maneuvers, evaluating at the same time their comprehensive effect on cardiovascular dynamics; the model response, resumed in Fig. 7, is coherent with available experimental data [23]. The comments are rather different in the case of pulsatile mechanical circulatory assistance when experiments were conducted using a physical model of an LVAD linked to the circulatory system in two different ways: atrioaortic and ventriculoaortic. During the discussed experiments, the physical LVAD was not a real device, as it was replaced by its electrical analog. Even though the used LVAD was a

**Table 1** Main circulatory parameter settings

Exp.	Left heart				Systemic circulation-1						Systemic circulation-2						Right heart				Pulmonary circulation									
	$E_{maxl}$	$V_0$	$C_{la}$	$L_s$	$R_{es}$	$C_{as}$	$R_{as}$	$C_{vs}$	$R_{vs}$	$Z_1$	$L_{a1}$	$R_{s1}$	$C_{a1}$	$L_{a2}$	$R_{s2}$	$C_{a2}$	$R_{ub1}$	$R_{ub2}$	$C_{ub}$	$R_{lb1}$	$R_{lb2}$	$C_{lb}$	$E_{maxr}$	$V_0$	$C_{ra}$	$L_p$	$R_{ep}$	$C_{ap}$	$R_{sup}$	$R_{vp}$
Caval occl.	4	5	30	-	-	-	-	-	0.67	13.3	1.7	0.07	9.3	0.3	2666	307	8	2933	8	89	1	5	30	0.47	20	1	80	4	5	
A-A-VAD	0.27	0	30	0.98	21	3.8	870/970	88	43/41	-	-	-	-	-	-	-	-	-	-	-	-	0.6	5	30	0.47	20	1	80	4	5
V-A-VAD	0.76/1.3	203/51	30	0.98	21	1.8	1092/1032	88	200/29	-	-	-	-	-	-	-	-	-	-	-	-	1.3/1	5	30	0.47	20	1	179/136	4	5

*Compliances (C) cm<sup>3</sup>·mmHg<sup>-1</sup>, resistances (R) g·cm<sup>-4</sup>·s<sup>-1</sup>, L-inertances (L) g·cm<sup>-4</sup>·s<sup>-1</sup>, L-inertances (L) g·cm<sup>-4</sup>·s<sup>-1</sup>, volumes (V) mmHg·cm<sup>-3</sup>, elastances (E) mmHg·cm<sup>-3</sup>, volumes (V) mmHg·cm<sup>-3</sup>, before/after ventricular assist device (VAD) onset, Systemic circulation-1 configuration used for VAD experiments, Systemic Circulation-2 configuration used for caval occlusion experiment, Caval occl. caval occlusion experiment, A-A-VAD atrioaortic connection LVAD experiment, V-A-VAD ventriculoaortic LVAD experiment*

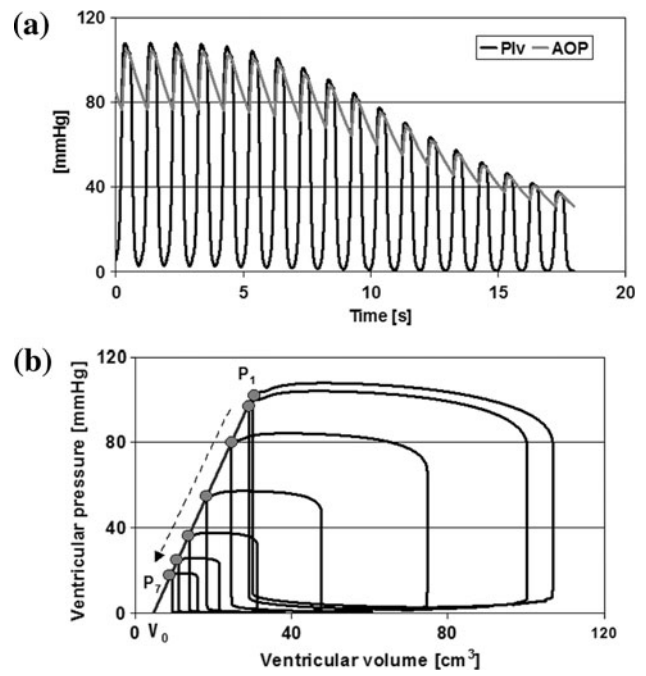


**Fig. 7** Caval occlusion experiment. **a** Time courses of ventricular and systemic arterial pressure. **b** Left ventricular  $p-v$  loops. Points  $P_1-P_7$ , corresponding to ventricular end-systolic pressure and rest volume  $V_0$  ( $5 \text{ cm}^3$ ), lie on a line with a slope equal to ventricular  $E_{max}$  ( $4 \text{ mmHg} \cdot \text{cm}^{-3}$ )

model, it was sufficient to demonstrate that the entire model can operate correctly merging two different environments: computational and physical–electrical. Results shown here, when compared with clinical or other experimental data (see Table 2), prove the correct response of the model and permit some further considerations on mechanical circulatory assistance. First, data sets used to fit simulated data correspond to two different assistance modes (atrioaortic and ventriculoaortic connection) and to two different circulatory conditions [8, 22]. In the case of atrioaortic connection assistance, experimental data were obtained from healthy sheep. In the case of ventriculoaortic connection assistance, clinical data were acquired before and 3 months after assistance onset: this implied the reconstruction of circulatory conditions twice, as it was not possible to assume that hemodynamic and ventricular parameters remained unchanged. In particular, the situation on the  $p-v$  plane, reported in [22], shows the scenario 3 months after LVAD assistance onset. This may imply a ventricular remodeling along with a general improvement of the state of the heart (Table 1) beyond the typical effects of ventriculoaortic connection assistance. This task was performed exploiting a feature of the model [10] that permits its tuning based on a limited set of input parameters. This kind of tuning procedure enabled us to estimate LV  $E_{max}$  and  $V_0$  in the two cases. Results of the procedure are reported in Table 2.



**Table 2** Comparison of left ventricular assist device (LVAD) literature data [8, 21] and simulation results

	HR (bpm <sup>-1</sup> )		CO (l·min <sup>-1</sup> )		AOP (mmHg)		LAP (mmHg)		P <sub>ap</sub> (mmHg)		CVP (mmHg)		ESV (cm <sup>3</sup> )		EDV (cm <sup>3</sup> )									
	1	2	%	1	2	%	1	2	%	1	2	%	1	2	%	1	2							
V-A																								
[21]	93	76	-18.3	4.47	5.89/2.1	+31.8	74	83	+12.2	27	10	-63	37	20	-45.9	13	7	-46.2	300	114	-62	357	164	-43.4
Simulation	93	76	-18.3	4.69	5.9/2.2	+30.2	78	89	+14.4	29	11	-62.4	39.8	21.5	-45.9	17.7	11.9	-32.8	295	116	-60.7	334	185	-44.6
A-A																								
[8]	127	131	+3	2.8	3/1.7	+7.1	36	43	+19.4	13	11	-15.4	17	16.7	-1.8	5.7	6.8	+19.3	-	-	-	-	-	-
Simulation	127	131	+3	2.9	3.2/1.65	+10.1	34.4	40.7	+14.9	14.3	12.8	-8.5	17.3	16.2	-6.2	5	5.4	+8.5	117	125	+8.6	140	137	-2.1

1 Before LVAD assistance onset, 2 after LVAD assistance onset, % percentage variation between 1 and 2, -/+ total cardiac output/LVAD flow, V-A ventriculoaortic connection LVAD assistance, A-A atrioaortic connection LVAD assistance

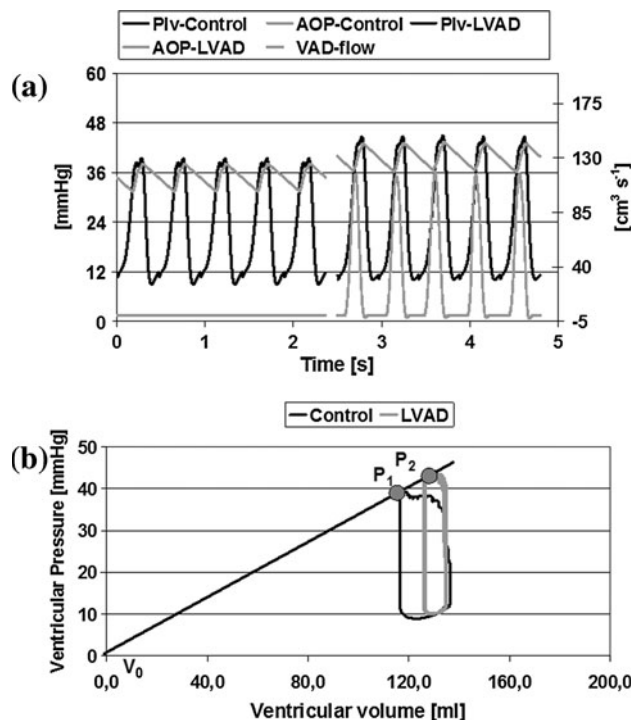


**Fig. 8** Atriaortic left ventricular assist device (LVAD) experiments. **a** Time courses of ventricular and aortic pressures and of LVAD output flow. The *left part* of the panel shows time courses before LVAD activation, whereas the *right part* of the same panel shows the corresponding time courses after LVAD activation. LVAD ejection is synchronized with LV ejection. **b** LV *p-v* loops before (*P*<sub>1</sub>) and during assistance (*P*<sub>2</sub>). The main effect of assistance is represented by a drop of ventricular external work and a rise in ventricular end-systolic volume

In general, the performed experiments evidence the basic difference between atrioaortic and ventriculoaortic connection assistance: analysis of Fig. 8 shows that the first nearly does not influence the position of the ventricular *p-v* loop but changes its width. As a consequence, cardiac mechanical efficiency [11] is not improved by this type of assistance. On the contrary, the main effect of the ventriculoaortic connection (Fig. 9) is a leftward shift of ventricular work cycle and rise in cardiac mechanical efficiency under the assistance. The situation was opposite when we analyzed ventricular external work variation [11]: in this case, it was the atrioaortic assistance that produced an evident drop in this variable. It must be emphasized that using a model permits consideration of several variables and their analysis separately and accurately.

**Study limitations**

The model described in this paper shows the possibility of merging two different environments with a resulting model behaving as a normal computational model. However, the

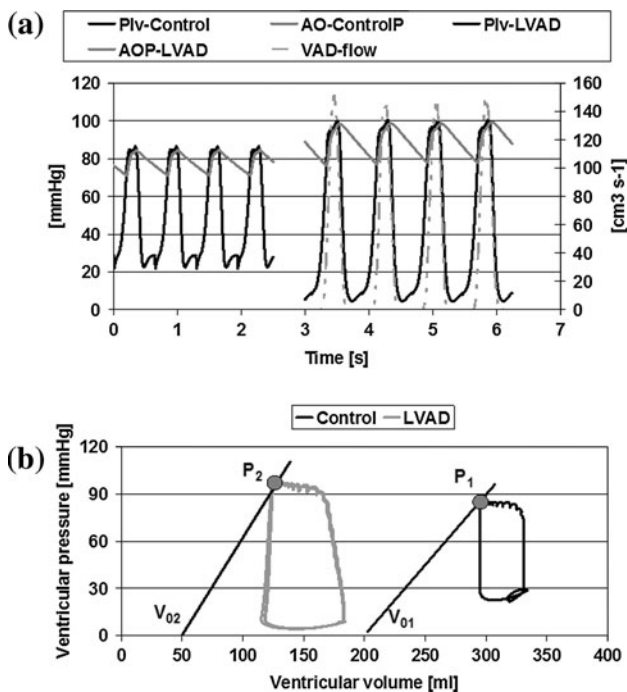


**Fig. 9** Ventriculoaortic connection left ventricular device (LVAD) experiments. **a** Time courses of ventricular and aortic pressures and of LVAD output flow. The *left part* of the panel shows the time courses before LVAD activation, whereas the *right part* of the same panel shows the corresponding time courses after LVAD activation. LVAD ejection is synchronized with LV ejection. **b** LV *p-v* loops before onset of ( $P_1$ ) and during assistance ( $P_2$ ). The effect of assistance consists of a rise in ventricular external work along and a drop in ventricular end-systolic volume. The two circulatory conditions were recorded before and after 6 months of going on assistance. The effect of the assistance induced ventricular remodelling, rising LV end-systolic elastance, and moving to the LV *p-v* loop

computational model was connected to an electrical physical section. Of course, despite the advantages due to the low cost and effectiveness in software development, hydraulic counterparts should replace electrical models. In general, the adopted methodology could be easily extended to merge computational and hydraulic environments. In this case, it will be necessary to adopt different interfaces, as was done using gear pumps [9] in the case of intra-aortic balloon pump (IABP) tests instead of voltage or current generators. It should be remarked that the IABP features imply the use of a hydraulic section in the model in which to insert the balloon: in this case, therefore, the computational–hydraulic model should be composed of an elastic tube mimicking the aorta, for balloon insertion, and of two interfaces for the computational model connection.

The use of an electrical model to represent an LVAD is clearly a limitation but has the undisputable advantage of demonstrating the possibility of interfacing in real time two different modeling environments and to prepare

implementation of the next computational–hydraulic application. The aim is not to replace a computational LVAD model with another model—electrical in this case. It is, rather, to demonstrate and verify exchange of information between two different environments. It should be considered that this exchange is based on A/D and D/A procedures that are exactly the same in computational/electrical and computational/hydraulic environments. A computational/electrical model, beyond its educational value, is much cheaper than the corresponding computational/hydraulic one. In fact, in the educational environment, it is sometimes too expensive or even impossible to use a real LVAD. An electrical model has the advantage, in comparison with a computational one, of permitting the evaluation of the operator’s response times due to the real-time operation provided by the entire system.

A prototype merging computational and hydraulic environments and designed to test any type of mechanical circulatory assistance, including nonpulsatile devices, is under development. Another critical issue of the model is the need to perform real-time simulations. The overall performance of the system could be significantly improved using the real-time version of LabVIEW.

### Conclusions

The modular computational circulatory model is able to react to the presence of mechanical circulatory assistance, reproducing the corresponding hemodynamic conditions. The model described in this paper is applied to pulsatile LVADs, but, in principle, it could be easily extended to the study of continuous flow pumps. It will be the next step in the model development. The software modular structure permits exploitation of the model for different computational and computational–physical applications [24]. Circulatory models can be useful tools for analyzing cardiovascular pathophysiology and, if adequately designed and constructed, could be successfully exploited in a variety of applications. One of the most appealing is the use of modeling to tailor assistance to a specific patient. This application is also pursued through the Integrated Project SensorART [25] funded by the European Union within the VII Framework Research Program.

Beyond research, the model could be usefully exploited in education and training, as it permits easy creation of realistic pathophysiological conditions with the use of different simulation modules. The future inclusion of autonomic control mechanisms, along with merging the circulatory and respiratory models, would bring the model closer to the concept of a virtual patient.

## Appendix

See Table 3.

**Table 3** Glossary of terms

Term <sub>maxr</sub>	Definition	Measurement
$E_{\max l}/E_{\max r}$	Left/right ventricular end-systolic elastance	mmHg cm <sup>-3</sup>
$V_{0l}/V_{0r}$	Left/right ventricular rest volume	cm <sup>3</sup>
$C_{1a}/C_{1ra}$	Left/right atrial compliance	cm <sup>3</sup> mmHg <sup>-1</sup>
$L_s/L_p$	Systemic/pulmonary inertance	g cm <sup>-4</sup>
$R_{cs}/R_{cp}$	Systemic/pulmonary characteristic resistance	g cm <sup>-4</sup> s <sup>-1</sup>
$C_{as}/C_{ap}$	Systemic/pulmonary arterial compliance	cm <sup>3</sup> mmHg <sup>-1</sup>
$R_{as}/R_{ap}$	Systemic/pulmonary arterial resistance	g cm <sup>-4</sup> s <sup>-1</sup>
$C_{vs}/C_{vp}$	Systemic/pulmonary venous compliance	cm <sup>3</sup> mmHg <sup>-1</sup>
$R_{vs}/R_{vp}$	Systemic/pulmonary venous resistance	g cm <sup>-4</sup> s <sup>-1</sup>
$L_{a1}$	Ascending aorta–aortic arch inertance	g cm <sup>-4</sup>
$R_{a1}$	Ascending aorta–aortic arch resistance	g cm <sup>-4</sup> s <sup>-1</sup>
$C_{a1}$	Ascending aorta–aortic arch compliance	cm <sup>3</sup> mmHg <sup>-1</sup>
$L_{a2}$	Thoracic–abdominal aorta inertance	g cm <sup>-4</sup>
$R_{a2}$	Thoracic–abdominal aorta resistance	g cm <sup>-4</sup> s <sup>-1</sup>
$C_{a2}$	Thoracic–abdominal aorta compliance	cm <sup>3</sup> mmHg <sup>-1</sup>
$R_{ub1}/R_{ub2}$	Upper body arterial/venous resistance	g cm <sup>-4</sup> s <sup>-1</sup>
$C_{ub}$	Upper body venous compliance	cm <sup>3</sup> mmHg <sup>-1</sup>
$R_{svc}$	Superior vena cava resistance	g cm <sup>-4</sup> s <sup>-1</sup>
$C_{svc}$	Superior vena cava compliance	cm <sup>3</sup> mmHg <sup>-1</sup>
$R_{lb1}/R_{lb2}$	Lower body arterial/venous resistance	g cm <sup>-4</sup> s <sup>-1</sup>
$C_{lb}$	Lower body venous compliance	cm <sup>3</sup> mmHg <sup>-1</sup>
$R_{ivc}$	Inferior vena cava resistance	g cm <sup>-4</sup> s <sup>-1</sup>
$C_{ivc}$	Inferior vena cava compliance	cm <sup>3</sup> mmHg <sup>-1</sup>
HR	Heart rate	beats min <sup>-1</sup>
$S/D$	Systole/diastole ratio	
CO	Cardiac output	l min <sup>-1</sup>
$AOP/P_{as}$	Aortic pressure	mmHg
$LAP/P_{1a}$	Left atrial pressure	mmHg
$P_{1v}$	Left ventricular pressure	mmHg
$P_{ap}$	Pulmonary arterial pressure	mmHg
CVP	Central venous pressure	mmHg
ESV	Ventricular end-systolic volume	cm <sup>3</sup>

**Table 3** continued

Term <sub>maxr</sub>	Definition	Measurement
EDV	Ventricular end-diastolic volume	cm <sup>3</sup>
$Q_{inVAD}/Q_{outVAD}$	Left ventricular input/output blood flow	ml s <sup>-1</sup>
$Q_{li}/Q_{lo}$	Left ventricular input/output blood flow	ml s <sup>-1</sup>
$Q_{vp}$	Pulmonary venous blood flow	ml s <sup>-1</sup>
$Q_{as}$	Systemic arterial blood flow	ml s <sup>-1</sup>
$Q_{cor}$	Total coronary blood flow	ml s <sup>-1</sup>
ESPVR	Ventricular end-systolic pressure–volume relationship	
GPIB	General purpose interface bus	
A/D–D/A	Analog to digital–digital to analog conversion	
Out var	Variable calculated in the computational environment and transmitted to the physical environment by D/A conversion	
In var	Variable calculated in the physical environment and transmitted to the computational environment by D/A conversion	

## References

- Zhou J, Armstrong GP, Medvedev AL, Smith WA, Golding LA, Thomas JD. Numeric modeling of the cardiovascular system with a left ventricular assist device. *ASAIO J.* 1999;45:83–9.
- Shi Y, Korakianitis T, Bowles C. Numerical simulation of cardiovascular dynamics with different types of VAD assistance. *J Biomech.* 2007;40:2919–33.
- Ferrari G, Kozarski M, De Lazzari C, Clemente F, Merolli M, Tosti G, Guaragno M, Mimmo R, Ambrosi D, Głapinski J. A hybrid (numerical-physical) model of the left ventricle. *Int J Artif Organs.* 2001;24:456–62.
- Balao LA, Boston JR, Antaki JF. Elastance-based control of a mock circulatory system. *Ann Biomed Eng.* 2001;29:244–51.
- Colacino FM, Arabia M, Danieli GA, Moscato F, Nicosia S, Piedimonte F, Valigi P, Pagnottelli S. Hybrid test bench for evaluation of any device related to mechanical cardiac assistance. *Int J Artif Org.* 2005;28:817–26.
- Gwak K-W, Paden BE, Noh MD, Antaki JF. Fluidic operational amplifier for mock circulatory systems. *IEEE Trans Con Syst Tech.* 2006;14:602–12.
- Ferrari G, De Lazzari C, Kozarski M, Clemente F, Górczyńska K, Mimmo R, Monnanni E, Tosti G, Guaragno M. A hybrid mock circulatory system: testing a prototype under physiologic and pathological conditions. *ASAIO J.* 2002;48:487–94.
- Colacino FM, Moscato F, Piedimonte F, Danieli G, Nicosia S, Arabia M. A modified elastance model to control mock ventricles in real-time: numerical and experimental validation. *ASAIO J.* 2008;54:563–73.
- Ferrari G, Kozarski M, De Lazzari C, Górczyńska K, Tosti G, Darowski M. Development of a hybrid (numerical-hydraulic) circulatory model: prototype testing and its response to IABP assistance. *Int J Artif Organs.* 2005;28:750–9.

10. Ferrari G, Kozarski M, Gu YJ, De Lazzari C, Di Molfetta A, Pałko KJ, Zieliński K, Górczyńska K, Darowski M, Rakhorst G. Application of a user friendly comprehensive circulatory model for hemodynamic and ventricular variables estimate. *Int J Artif Organs*. 2008;31:1043–54.
11. Sagawa K, Maughan L, Suga H, Sunagawa K. Cardiac contraction and the pressure–volume relationship. New York: Oxford University Press; 1988.
12. Campbell KB, Kirkpatrick RD, Knowlen GG, Ringo JA. Late-systolic pumping properties of the left ventricle. Deviation from elastance-resistance behaviour. *Circ Res*. 1990;66:218–33.
13. Gilbert JC, Glantz SA. Determinants of left ventricular filling and of the diastolic pressure-volume relation. *Circ Res*. 1989;64:827–52.
14. Korakianitis T, Shi Y. A concentrated parameter model for the human cardiovascular system including heart valve dynamics and atrioventricular interaction. *Med Eng Phys*. 2006;28:613–28.
15. Di Molfetta A, Cesario M, Tota C, Santini L, Forleo GB, Sgueglia M, Ferrari G, Romeo F. Use of a comprehensive numerical model to improve biventricular pacemaker temporization in patients affected by heart failure undergoing to CRT-D therapy. *Med Biol Eng Comput*. 2010;48:755–64.
16. Heldt T, Shim EB, Kamm RD, Mark RG. Computational modeling of cardiovascular response to orthostatic stress. *J Appl Physiol*. 2002;92:1239–54.
17. Avolio AP. Multi-branched model of the human arterial system. *Med Biol Eng Comput*. 1980;18:709–18.
18. Downey JM, Kirk ES. Inhibition of coronary blood flow by a vascular waterfall mechanism. *Circ Res*. 1975;36:753–60.
19. Darowski M, De Lazzari C, Ferrari G, Clemente F, Guaragno M. Computer simulation of hemodynamic parameter changes by mechanical ventilation and biventricular circulatory support. *Methods Inf Med*. 2000;39:332–8.
20. Ferrari G, Kozarski M, De Lazzari C, Górczyńska K, Mimmo R, Guaragno M, Tosti G, Darowski M. Modelling of cardiovascular system: development of a hybrid (numerical-physical) model. *Int J Artif Organs*. 2003;26:1104–14.
21. Kozarski M, Ferrari G, Zieliński K, Górczyńska K, Pałko KJ, Tokarz A, Darowski M. A new hybrid electro-numerical model of the left ventricle. *Comput Biol Med*. 2008;38:979–89.
22. Haft J, Armstrong W, Dyke DB, Aaronson KD, Koelling TM, Farrar DJ, Pagani FD. Hemodynamic and exercise performance with pulsatile and continuous-flow left ventricular assist devices. *Circulation*. 2007;116(Suppl):I8–15.
23. Baan J, van der Velde ET, de Bruin HG, Smeenk GJ, Koops J, van Dijk AD, Temmerman D, Senden J, Buis B. Continuous measurement of left ventricular volume in animals and humans by conductance catheter. *Circulation*. 1984;70:812–23.
24. Ferrari G, Kozarski M, De Lazzari C, Górczyńska K, Pałko KJ, Zieliński K, Di Molfetta A, Darowski M. Role and applications of circulatory models in cardiovascular pathophysiology. *Biocybern Biomed Eng*. 2009;29:3–24.
25. SensorART—A remote controlled Sensorized ARTificial heart enabling patients empowerment and new therapy approaches—Integrated Project funded within the framework of the European Community's Seventh Framework Programme (FP7/2007–2013) under grant agreement no. 248763. (<http://www.sensorart.eu>).